



Ultrafast manipulation of the weakly bound helium dimer

Maksim Kunitski¹, Qingze Guan^{2,3}, Holger Maschkiwitz¹, Jörg Hahnenbruch¹, Sebastian Eckart¹, Stefan Zeller^{1,4}, Anton Kalinin⁴, Markus Schöffler¹, Lothar Ph. H. Schmidt¹, Till Jahnke¹, Dörte Blume^{2,3} and Reinhard Dörner¹

Controlling the interactions between atoms with external fields opened up new branches in physics ranging from strongly correlated atomic systems to ideal Bose¹ and Fermi² gases and Efimov physics^{3,4}. Such control usually prepares samples that are stationary or evolve adiabatically in time. In contrast, in molecular physics, external ultrashort laser fields are used to create anisotropic potentials that launch ultrafast rotational wave packets and align molecules in free space5. Here we combine these two regimes of ultrafast times and low energies. We apply a short laser pulse to the helium dimer, a weakly bound and highly delocalized single bound state quantum system. The laser field locally tunes the interaction between two helium atoms, imparting an angular momentum of 2h and evoking an initially confined dissociative wave packet. We record a video of the density and phase of this wave packet as it propagates from small to large internuclear distances. At large internuclear distances, where the interaction between atoms is negligible, the wave packet is essentially free. This work paves the way for future tomography of wave-packet dynamics and provides the technique for studying exotic and otherwise hardly accessible quantum systems, such as halo and Efimov states.

In ultracold atomic gas experiments, the two-body interaction is commonly tuned by an external magnetic field in the vicinity of a Feshbach resonance^{6,7}. An alternative approach is to use an external electric field8, which is particularly interesting for weakly bound systems that consist of non-magnetic atoms, in which the interaction between field-induced dipoles can notably alter the native interatomic potential. One such system is the helium dimer, ⁴He₂, in which the two helium atoms are held together by an extremely weak van der Waals interaction. The corresponding potential is isotropic with a well depth of 11 K (0.95 meV) at an internuclear distance of 2.97 Å (Fig. 1a,c) (ref. 9). In the absence of external fields, the potential supports a single rovibrational bound state with a tiny binding energy of 1.7 mK (150 neV) (ref. 10). The probability distribution of the state is isotropic and spreads far beyond the potential well, so that about 80% of the dimer resides in the classically forbidden tunnelling region, justifying the name 'quantum halo'.

A number of theory predictions exist on exciting new phenomena that arise from the field modification of the interaction between two helium atoms. They range from the tunability of rovibrational states^{11–14} (see refs. ^{15–21} for similar effects in alkali molecules) to the emergence of a 'covalent'-like dimer that supports many bound states^{13,22}. In the three-body sector, the creation of an infinite tower

of field-induced ⁴He³He² Efimov trimers was predicted in the seminal work by Nielsen et al.²³. However, these phenomena are unexplored experimentally, owing to challenges such as the realization of high field strengths and the preparation and efficient detection of such fragile quantum states. In particular, the following open questions have motivated the current work. How does the quantum halo respond to the non-adiabatic and anisotropic tuning of the interatomic interaction? Does it react to the field as a whole and start to rotate, as a common rigid molecule would? Is an angular anisotropy observed, even though the native He–He potential does not support rotationally excited bound states?

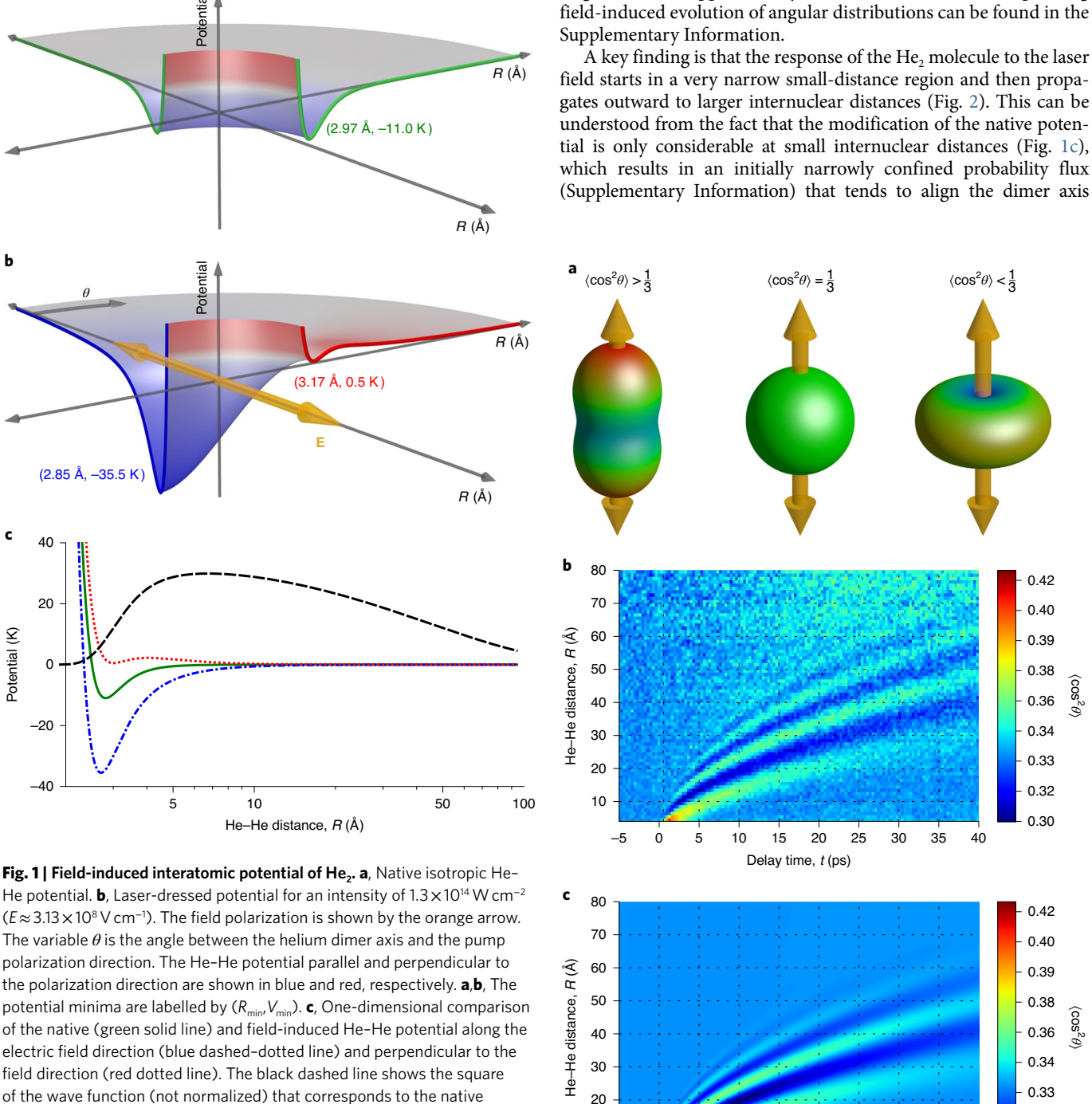
We apply a strong laser field to the helium dimer and make a video of the dimer's response using time-resolved Coulomb explosion imaging. We find that the electric field launches a dissociative wave packet at small internuclear distances by locally modifying the He–He interaction potential (Fig. 1b,c). The wave packet propagates towards larger internuclear distances, where it becomes essentially free, which results in a time-dependent alignment signal (angular anisotropy). Interference of this free wave packet with the residual isotropic ground-state wave function allows for the observation of the quantum phase of the wave packet.

Helium dimers in a mass-selected supersonic ter beam²⁴ are irradiated with a 310 fs 780 nm pump laser pulse with a volume-averaged intensity of 1.3×10¹⁴ W cm⁻² $(E \approx 3.13 \times 10^8 \,\mathrm{V \, cm^{-1}})$, which produces a negligible amount of ionization. Owing to the anisotropic dipole polarizability, this strong laser field introduces an angle dependence into the He-He interaction. The induced potential is repulsive along the perpendicular direction and its depth along the polarization direction is about three times deeper than that of the native potential (Fig. 1b,c). This response to the external electric field distinguishes the He₂ molecule notably from common covalently bound rigid molecules²⁵, in which the laser field induces a tiny overall attractive anisotropy. The pump pulse is followed by a delayed and much stronger 30 fs probe pulse (approximately 10^{16} W cm⁻² in intensity), which ionizes both helium atoms. The two ions are subsequently driven apart by their mutual Coulomb repulsion, which results in the so-called Coulomb explosion, which is imaged by a cold target recoil ion momentum spectroscopy reaction microscope^{26,27} (Supplementary Information). This imaging yields the internuclear distance and the orientation of individual dimers at the instant of ionization by the probe pulse.

The response of a diatomic molecule to a laser field can be quantified by the alignment merit, $\cos^2\theta$, where θ is the angle between the internuclear axis and the polarization direction of the pump

Institut für Kernphysik, Goethe-Universität Frankfurt am Main, Frankfurt, Germany. ¹Homer L. Dodge Department of Physics and Astronomy, University of Oklahoma, Norman, OK, USA. ³Center for Quantum Research and Technology, University of Oklahoma, Norman, OK, USA. ⁴GSI − Helmholtzzentrum für Schwerionenforschung, Darmstadt, Germany. ⊠e-mail: kunitski@atom.uni-frankfurt.de; doerner@atom.uni-frankfurt.de

NATURE PHYSICS



20

10

-5

laser. Initially, the He₂ molecule is in a pure s-state with an isotropic angular distribution at all internuclear distances. This corresponds to the expectation value of $\cos^2\theta$, $\langle\cos^2\theta\rangle = 1/3$ (Fig. 2). About 1 ps after the application of the 310 fs laser pulse (pump), we observe a partial alignment along the polarization direction of the pump field at small internuclear distances ($\langle \cos^2 \theta \rangle \approx 0.42$, Fig. 2b), although the far-out regions of the wave function are still isotropic. The alignment wave evolves towards larger internuclear distances such that, for a delay time of 40 ps, the inner part of the wave function has restored its spherical symmetry while the outer part (30-70 Å) displays R-dependent alignment. The experimental alignment evolution is well reproduced by our parameter-free theory calculation

potential. Note the logarithmic scale on the x axis.

A key finding is that the response of the He, molecule to the laser field starts in a very narrow small-distance region and then propagates outward to larger internuclear distances (Fig. 2). This can be understood from the fact that the modification of the native potential is only considerable at small internuclear distances (Fig. 1c),

(Fig. 2c and Supplementary Information). The corresponding

which results in an initially narrowly confined probability flux (Supplementary Information) that tends to align the dimer axis

Fig. 2 | Temporal evolution of field-induced alignment. a, Schematic of the angular distribution of the dimer axis with respect to the laser field polarization (orange arrows) for different expectation values of $\cos^2\theta$. The density changes in angular distributions are visualized by colour. **b**, Expectation value of $\cos^2\theta$ (colour coded) as function of the internuclear distance R and the delay time t between the pump and probe pulses. **c**, Quantum calculation for the same parameters as in the experiment. Theoretical probabilities were convolved with Gaussian functions of variable width prior to the calculation of $\cos^2\theta$ to emulate the R-dependent experimental resolution (Supplementary Information).

20 25 30 35 40

10

15 Delay time, t (ps) 0.32

0.30

LETTERS NATURE PHYSICS

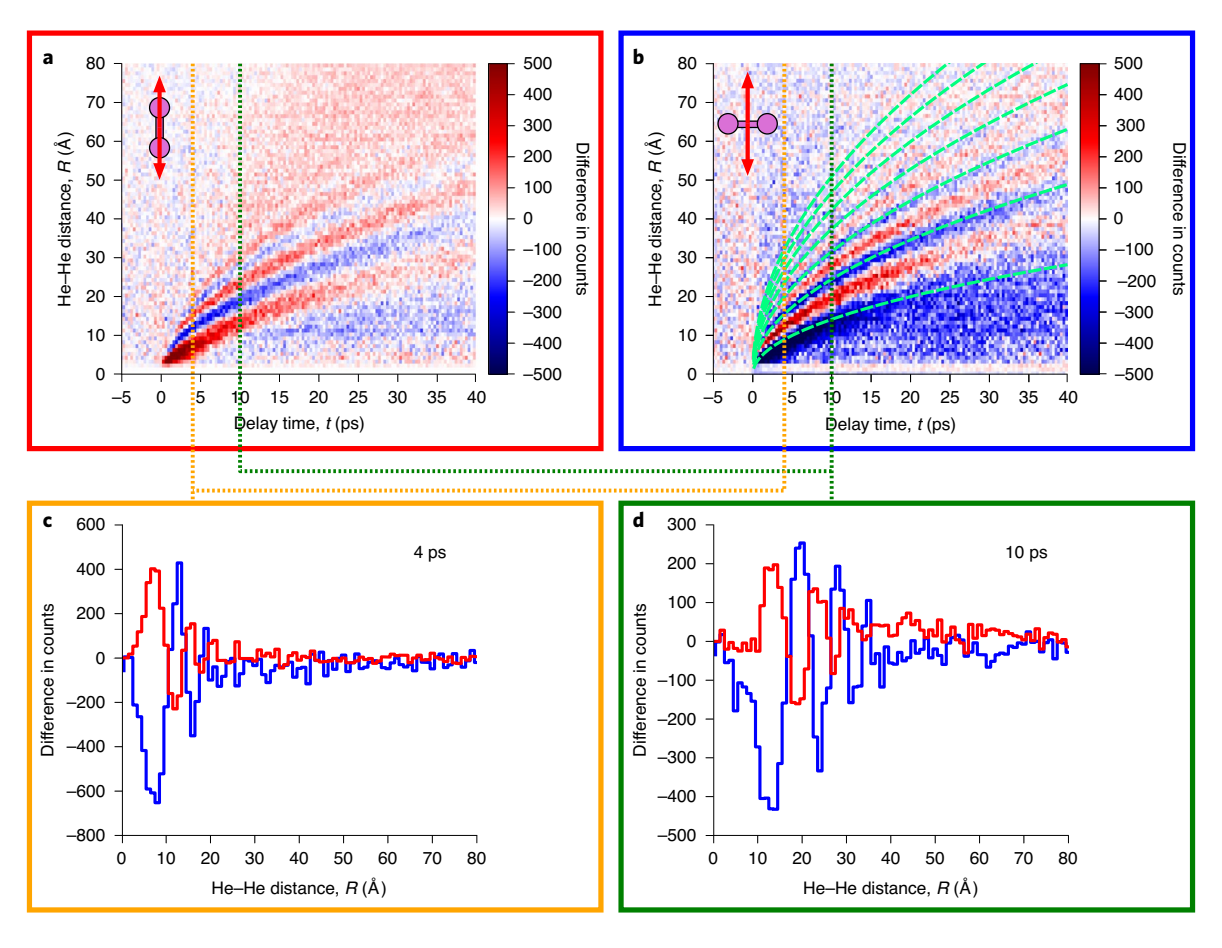


Fig. 3 | Time evolution of the dissociative wave packet in He_2 after the laser 'kick'. a,b, Experimentally determined change of probability $2\pi R^2 \left(|\Psi_{\text{obs}}(\mathbf{R},t)|^2 - |\Psi_{\text{GS}}(R)|^2 \right)$ (colour coded as the difference in counts) as a function of the internuclear distance R and the delay time t for the cases in which the dimer axis is parallel to the pump polarization (a) and perpendicular to the pump polarization (b). To make the plots, we consider $\theta = 0 \pm 40^\circ$ (a; Supplementary Information) and $\theta = 90 \pm 40^\circ$ (b). The green dashed lines in b show the calculated constant-phase evolution of a free particle with a reduced mass of 2 AMU (Supplementary Information). The sketches show the relative orientation of the dimer axis with respect to the laser field polarization (shown by a red double arrow). c,d, To highlight the difference between the probability change for $\theta = 0^\circ$ and $\theta = 90^\circ$, the red and blue lines show fixed-R cuts through the data shown in a and b, respectively, for delay times of 4 ps (c, orange dotted vertical lines in a and b) and 10 ps (d, green dotted vertical lines in a and b).

along the field. Owing to the large extent of the initial-state wave function, the helium dimer does not react as a whole to such a localized 'kick'. This is completely different from what is known from all alignment experiments performed to date, in which molecules respond to the laser 'kick' as a single unit and therefore can be treated within the (semi-) rigid rotor approximation⁵. This response is commonly understood as a coherent excitation of many rotational bound states; that is, the emergence of a rotational wave packet. The temporal evolution of such a wave packet results in a distance-independent but time-periodic alignment signal. The field-free He–He interaction potential, by contrast, does not support any rotationally excited bound states, and the He₂ wave-packet dynamics, which is characterized by a strong coupling of the rotational and vibrational degrees of freedom, involves the dissociation continuum.

Another way of looking at the field-induced dynamics is to visualize the He₂ density. The modifications of the probability distribution that are induced by the pump laser for $\theta \approx 0^{\circ}$ and for $\theta \approx 90^{\circ}$ are shown as functions of the internuclear distance R and the delay time t in Fig. 3a,b. Remarkably, our measurement allows for the phase of the outward propagating density wave to be resolved.

In quantum mechanics, the phase of the time-dependent wave packet can be observed only by letting different wave-packet portions interfere, which is the basis for any kind of interferometry^{28,29}.

As the ground-state wave function $\Psi_{GS}(R)$ of the helium dimer extends to large internuclear distances, it provides a real-valued, unstructured and isotropic quantum background with which the outgoing dissociative wave-packet portion can interfere, thereby unveiling the quantum phase. Writing the observed time-dependent wave packet $\Psi_{\text{obs}}(\mathbf{R},t)$ as a superposition of partial waves, $\Psi_{\text{obs}}(\mathbf{R},t) = \sum_{J=0,2,...} \psi_J(R,\theta,t)$ with $\psi_J(R,\theta,t) = R^{-1}u_J(R,t)Y_{J0}(\theta)$ (*J* is

the orbital angular momentum quantum number, $u_j(R,t)$ are partial wave components and $Y_{j0}(\theta)$ are spherical harmonics), the density modifications are, to leading order, described by

$$2\pi R^{2} (|\Psi_{\text{obs}}(\mathbf{R},t)|^{2} - |\Psi_{\text{GS}}(R)|^{2}) \approx 4\pi R \Psi_{\text{GS}}(R) |u_{2}(R,t)|Y_{20}(\theta) \cos(\gamma_{2}(R,t)),$$
(1)

where $\gamma_2(R,t)$ is the position- and time-dependent phase of the wave packet (Supplementary Information). The $\cos(\gamma_2(R,t))$ dependence and, correspondingly, the finger-like structures in Figs. 2b,c and 3a,b are a direct consequence of the fact that the dissociating J=2 partial wave component is interfering with the J=0 partial wave component (Supplementary Video 1).

The $\theta = 0^{\circ}$ and $\theta = 90^{\circ}$ waves are out of phase (Fig. 3c,d). This is in agreement with equation (1), which states that the density

NATURE PHYSICS LETTERS

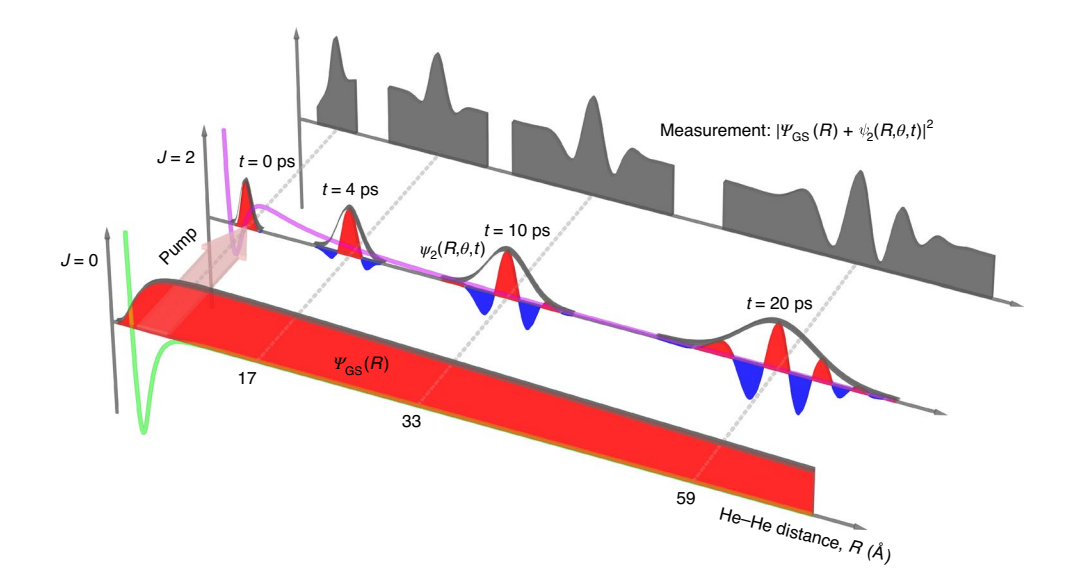


Fig. 4 | Schematic of radial response of the highly delocalized single-state helium dimer to a strong laser field (pump). At t=0 ps, the pump field transfers a tiny part of the ground-state wave function $\Psi_{GS}(R)$ at small internuclear distances to the dissociative J=2 potential (as indicated by the red arrow). The evolution of this dissociative wave packet, which consists mainly of the partial wave $\psi_2(R,\theta,t)$, is imaged by Coulomb explosion imaging. The phase of the wave packet is resolved owing to its interference with the spatially extended J=0 ground-state wave function $\Psi_{GS}(R)$. Red and blue colours correspond to the positive and negative values, respectively, of the real part of $\Psi_{GS}(R)$ and $\psi_2(R,\theta,t)$. The radial part of the partial wave $\psi_2(R,\theta,t)$ shown here is characterized by the determined group velocity of about 2.6 Å ps⁻¹, but is, for illustrative purposes, less dispersive than the true wave packet. Dotted grey lines are guides to the eye. The ground (J=0) and the dissociative (J=2) potentials are shown in green and pink, respectively. The interference of the dissociative wave packet with the ground-state wave function $\Psi_{GS}(R)$ is shown by shaded grey regions.

modulations at different θ but at fixed R and delay time t differ by the value of Y_{20} , which gives $Y_{20}(\theta=0^\circ)=-2Y_{20}(\theta=90^\circ)$. The fact that the pump laser under our experimental conditions populates predominantly the J=0 and J=2 partial waves explains why two observables, namely, alignment (Fig. 2) and changes of the probability distribution (Fig. 3), show similar dynamics.

As the He–He interaction potential (Fig. 1a) can be neglected at large internuclear distances, the unbound part of the wave packet (Fig. 3a,b) describes a quantum particle that moves freely without the influence of any forces. Therefore, our experiment directly visualizes the temporal evolution of a propagating free-particle wave packet with the otherwise unobservable quantum phase.

The observed response of a single-state quantum halo, He₂, to an intense short electric field can be summarized as follows (Fig. 4). The laser field 'grabs on' to a small portion of the ground-state wave function of He2 at small internuclear distances and transfers a small fraction of the ground-state population to the repulsive J=2 potential, which creates a localized dissociative wave packet in the continuum. During the subsequent time evolution of the wave packet, the potential energy is converted to kinetic energy. Concurrently, the envelope of the wave packet spreads with time owing to the intrinsic dispersion of the matter wave. At large internuclear distances, where the interaction potential is negligible, the wave-packet evolution resembles that of a free quantum particle with a mean group velocity of about 2.6 Å ps⁻¹ (Supplementary Information). Not only the envelope, but also the phase of this J = 2 wave packet is accessible during the measurement owing to its interference with the spatially extended isotropic J=0 ground-state wave function $\Psi_{GS}(R)$.

The results reported here provide experimental evidence that the $^4\text{He}_2$ potential can be tuned through the application of an external electric field. Largely delocalized universal quantum systems such as the helium dimer open new avenues of investigation for wave-packet interferometry. These systems have rather simple ground states of a huge spatial extent, which are frequently described by effective low-energy theories. Such initial states can serve as a reference

background with which dissociative wave-packet portions, launched by a short and intense laser pulse, can interfere. Then, imaging of the corresponding superposition state reveals directly the temporal evolution of the amplitude and quantum phase of the wave packet. This technique, which combines universal low-energy physics with short high-intensity pulses, can be extended to few-body quantum systems such as the helium trimer, in which the field-induced dynamics is completely unexplored. The strong electric field can be used also to create superpositions of bound states in quantum systems³⁰. An exciting example experiment would be to create a superposition of the ground state and excited Efimov state of He₃ and to watch the birth and decay of an Efimov state in time.

Online content

Any methods, additional references, Nature Research reporting summaries, source data, extended data, supplementary information, acknowledgements, peer review information; details of author contributions and competing interests; and statements of data and code availability are available at https://doi.org/10.1038/s41567-020-01081-3.

Received: 15 April 2020; Accepted: 12 October 2020; Published online: 21 December 2020

References

- Anderson, M. H., Ensher, J. R., Matthews, M. R., Wieman, C. E. & Cornell, E. A. Observation of Bose–Einstein condensation in a dilute atomic vapor. Science 269, 198–201 (1995).
- DeMarco, B., Bohn, J. L., Burke, J. P., Holland, M. & Jin, D. S. Measurement of p-wave threshold law using evaporatively cooled fermionic atoms. *Phys. Rev. Lett.* 82, 4208–4211 (1999).
- 3. Efimov, V. Energy levels arising from resonant two-body forces in a three-body system. *Phys. Lett. B* **33**, 563–564 (1970).
- Kraemer, T. et al. Evidence for Efimov quantum states in an ultracold gas of caesium atoms. *Nature* 440, 315–318 (2006).
- Stapelfeldt, H. & Seideman, T. Colloquium: Aligning molecules with strong laser pulses. Rev. Mod. Phys. 75, 543–557 (2003).

LETTERS NATURE PHYSICS

- Chin, C., Grimm, R., Julienne, P. & Tiesinga, E. Feshbach resonances in ultracold gases. Rev. Mod. Phys. 82, 1225–1286 (2010).
- Kotochigova, S. Controlling interactions between highly magnetic atoms with Feshbach resonances. Rep. Prog. Phys. 77, 093901 (2014).
- Kurizki, G., Mazets, I. E., O'Dell, D. H. J. & Schleich, W. P. Bose–Einstein condensates with laser-induced dipole-dipole interactions beyond the mean-field approach. *Int. J. Mod. Phys. B* 18, 961–974 (2004).
- Cencek, W. et al. Effects of adiabatic, relativistic, and quantum electrodynamics interactions on the pair potential and thermophysical properties of helium. J. Chem. Phys. 136, 224303 (2012).
- Zeller, S. et al. Imaging the He₂ quantum halo state using a free electron laser. Proc. Natl Acad. Sci. USA 113, 14651–14655 (2016).
- Friedrich, B., Gupta, M. & Herschbach, D. Probing weakly-bound species with nonresonant light: dissociation of He₂ induced by rotational hybridization. Collect. Czech. Chem. Commun. 63, 1089–1093 (1998).
- Lemeshko, M. & Friedrich, B. Probing weakly bound molecules with nonresonant light. *Phys. Rev. Lett.* 103, 053003 (2009).
- Wei, Q., Kais, S., Yasuike, T. & Herschbach, D. Pendular alignment and strong chemical binding are induced in helium dimer molecules by intense laser fields. Proc. Natl Acad. Sci. USA 115, E9058–E9066 (2018).
- Guan, Q. & Blume, D. Electric-field-induced helium-helium resonances. Phys. Rev. A 99, 033416 (2019).
- Lemeshko, M. & Friedrich, B. Fine-tuning molecular energy levels by nonresonant laser pulses. J. Phys. Chem. A 114, 9848–9854 (2010).
- Aganoglu, R., Lemeshko, M., Friedrich, B., González-Férez, R. & Koch, C. Controlling a diatomic shape resonance with non-resonant light. Preprint at https://arxiv.org/abs/1105.0761 (2011).
- Lemeshko, M. Shaping interactions between polar molecules with far-off-resonant light. Phys. Rev. A 83, 051402 (2011).
- González-Férez, R. & Koch, C. P. Enhancing photoassociation rates by nonresonant-light control of shape resonances. *Phys. Rev. A* 86, 063420 (2012).
- Lemeshko, M., Krems, R. V., Doyle, J. M. & Kais, S. Manipulation of molecules with electromagnetic fields. *Mol. Phys.* 111, 1648–1682 (2013).

- 20. Tomza, M. et al. Interatomic potentials, electric properties and spectroscopy of the ground and excited states of the Rb₂ molecule: ab initio calculations and effect of a non-resonant field. *Mol. Phys.* 111, 1781–1797 (2013).
- Crubellier, A., González-Férez, R., Koch, C. P. & Luc-Koenig, E. Asymptotic model for shape resonance control of diatomics by intense non-resonant light: universality in the single-channel approximation. *New J. Phys.* 17, 045020 (2015).
- Balanarayan, P. & Moiseyev, N. Strong chemical bond of stable He₂ in strong linearly polarized laser fields. *Phys. Rev. A* 85, 032516 (2012).
- Nielsen, E., Fedorov, D. V. & Jensen, A. S. Efimov states in external fields. *Phys. Rev. Lett.* 82, 2844–2847 (1999).
- Schöllkopf, W. & Toennies, J. P. Nondestructive mass selection of small van der Waals clusters. Science 266, 1345–1348 (1994).
- Maroulis, G., Makris, C., Hohm, U. & Goebel, D. Electrooptical properties and molecular polarization of iodine, I₂. J. Phys. Chem. A 101, 953–956 (1997)
- Ullrich, J. et al. Recoil-ion and electron momentum spectroscopy: reaction-microscopes. Rep. Prog. Phys. 66, 1463 (2003).
- Jagutzki, O. et al. Multiple hit readout of a microchannel plate detector with a three-layer delay-line anode. *IEEE Trans. Nucl. Sci.* 49, 2477–2483 (2002).
- Christian, J. F., Broers, B., Hoogenraad, J. H., van der Zande, W. J. & Noordam, L. D. Rubidium electronic wavepackets probed by a phase-sensitive pump-probe technique. *Opt. Commun.* 103, 79–84 (1993).
- Kunitski, M. et al. Double-slit photoelectron interference in strong-field ionization of the neon dimer. Nat. Commun. 10, 1 (2019).
- Yudkin, Y., Elbaz, R., Giannakeas, P., Greene, C. H. & Khaykovich, L. Coherent superposition of Feshbach dimers and Efimov trimers. *Phys. Rev. Lett.* 122, 200402 (2019).

Publisher's note Springer Nature remains neutral with regard to jurisdictional claims in published maps and institutional affiliations.

© The Author(s), under exclusive licence to Springer Nature Limited 2020

NATURE PHYSICS LETTERS

Data availability

All experimental data has been archived at the Goethe-University of Frankfurt am Main and is available upon request. Source data are provided with this paper.

Acknowledgements

We thank B. Friedrich for inspiring this work over many years and M. Lemeshko for many helpful discussions and calculations. The experimental work was supported by Deutsche Forschungsgemeinschaft (DFG). This work used the OU Supercomputing Center for Education and Research (OSCER) at the University of Oklahoma. Q.G. and D.B. acknowledge support by the US National Science Foundation (grant no. PHY-1806259).

Author contributions

M.K., H.M., J.H., S.E., S.Z., A.K., M.S., L.P.H.S. and T.J. contributed to the experiment. M.K. and R.D. analysed the experimental data. Q.G. and D.B.

developed the theory. Q.G. performed the calculations. All authors contributed to the manuscript.

Competing interests

The authors declare no competing interests.

Additional information

Supplementary information is available for this paper at https://doi.org/10.1038/s41567-020-01081-3.

Correspondence and requests for materials should be addressed to M.K. or R.D.

Peer review information *Nature Physics* thanks Daniel Rolles and the other, anonymous, reviewer(s) for their contribution to the peer review of this work.

Reprints and permissions information is available at www.nature.com/reprints.